NANO LETTERS

2007
Vol. 7, No. 1
101−107

Onset of Plasticity in Gold Nanopillar Compression

Eugen Rabkin*,†,‡ and David J. Srolovitz‡,§

Department of Materials Engineering, Technion-Israel Institute of Technology, 32000 Haifa, Israel, Department of Physics, Yeshiva University, 500 West 185th Street, New York, New York 10033, and Department of Mechanical & Aerospace Engineering, Princeton University, Princeton, New Jersey 08540

Received September 22, 2006; Revised Manuscript Received November 8, 2006

ABSTRACT

On the basis of a series of molecular dynamics simulations of the compressive deformation of ⟨111⟩-oriented gold nanopillars, we demonstrate that slip nucleates at surface features for which the amplitude of thermal vibrations is a maximum. This leads to a yield stress which can be either a linear or parabolic function of temperature, depending on the strength with which atoms are bound to the surface. Changing the surface structure by removing weakly bound atoms produces a striking rise in yield strength and a change in its temperature dependence.

In recent years it has been established that the plastic deformation mechanisms of sub-micrometer metallic objects are very different from those of bulk metals and alloys. Mechanical testing of metallic nanowires[1] and micromachined cantilever microbeams[2] revealed that the yield stress and strength of small objects increases with decreasing geometric dimension. While in nanocrystalline metals, processes at grain boundaries (nucleation of dislocations and grain boundary sliding) play an important role in plasticity,[3] in small single crystalline samples slip nucleates either heterogeneously at free surfaces or homogeneously in the crystal. The latter process plays an important role in the presence of high stress gradients, i.e., during nanoindentation.[4]

Recently, Nix and co-workers[5,6] developed an elegant microcompression method for homogeneous compression of sub-micrometer-scale metallic structures. They found that the flow stress of single crystalline gold pillars homogeneously compressed along ⟨100⟩ increases significantly with decreasing pillar diameter, reaching 4 GPa for a 300 nm diameter pillar.[6] For comparison, the yield strength of bulk, annealed gold is ∼30 MPa at 2% strain.[7] To interpret this strong size effect, Nix and co-workers proposed a "Dislocation Starvation" hypothesis. They suggested that below a critical diameter, the traditional dislocation multiplication mechanisms that lead to work hardening stop operating and dislocations freely traverse the sample. Under such dislocation-starved conditions, continuing plastic deformation is only possible if the applied stress is sufficiently large to nucleate new dislocations. Therefore, the process of dislocation nucleation, either at nanomaterial surfaces or interiors, plays a fundamental role in determining nanomaterial strength within the "Dislocation Starvation" regime.

The homogeneous tensile/compressive plastic deformation of metallic nanowires in the geometry similar to that employed in refs 5 and 6 has been a subject of a number of recent molecular dynamics (MD) computer simulation studies.[8,9] These simulations confirmed that defect-free nanowires exhibit yield stresses in the gigapascal range. However, both the location of dislocation nucleation and the mechanisms by which dislocations nucleate still remain the subjects of controversy. It was shown that a stacking fault (SF) traversing the whole cross section of a nanowire[8] and a full atomic step at the side surface of a nanowire[9] significantly reduce the nanowire yield stress. This is not surprising, since it is known that surface steps normal to the loading direction cause stress concentration in their vicinity and are preferential sites for dislocation nucleation.[10] Diao et al. observed that slip nucleates at the edges of the nanowires of rectangular cross section,[8] while in the simulation of Hyde et al. of twinned circular nanowires with a bamboo microstructure slip always nucleated at the triple junctions between the twin boundary and the nanowire surface.[9] Since neither sharp edges running parallel to the loading direction nor the twin/surface intersections are effective stress concentrators, these observations imply that slip nucleation in nanowires is essentially a surface phenomenon. Diao et al. noted that even when nanowires are deformed in compression, the atoms on or near the surface are under large *tensile* atomic stress (even

* Corresponding author. Email: erabkin@tx.technion.ac.il
† Department of Materials Engineering, Technion-Israel Institute of Technology.
‡ Department of Mechanical & Aerospace Engineering, Princeton University.
§ Department of Physics, Yeshiva University.

10.1021/nl0622350 CCC: $37.00
Published on Web 12/14/2006

during yielding). This tensile stress is associated with the surface stresses. Because of the presence of these large tensile stresses at the surface during compressive deformation, it was argued that the actual dislocation nucleation occurs in the interior of the nanowire, where the atomic stresses are homogeneous and compressive (dislocations nucleated at the tensile surface would be pushed back to the surface if they entered the compressive bulk). If dislocations are nucleated in the interior of the nanowire, a critical resolved shear stress (CRSS) would apply.[8]

In the present study, we clarify the factors that control slip nucleation during compression of single crystalline gold nanowires/nanopillars. We perform a series of atomistic simulations of nanopillar compression with two embedded atom method (EAM) potentials for gold.[11,12] The EAM potential of Cai and Ye (CY)[11] has been employed in earlier studies of plastic deformation of gold asperities[13] but yields surface and SF energies of gold that are significantly smaller than those found experimentally. The recently developed potential of Grochola et al. (GRS)[12] gives more realistic surface and SF energies. A detailed comparison of the two EAM potentials can be found in ref 14. In order to clarify the nature of the dislocation nucleation mechanism, we emphasize the temperature dependence of the yield stress.

Our MD simulations were performed with a constant number of atoms under isothermal conditions (using the Nosé-Hoover thermostat[15]). The simulation time step was fixed at 5 fs. The computational cell was constructed by carving a cylinder of a radius $R = 12a$ from a bulk face-centered cubic (fcc) crystal, where a is the lattice parameter (see Figure 1a). The initial value of a was chosen to be that of the bulk solid at the temperature where the simulation was performed. Periodic boundary conditions were imposed along the cylinder axis z, while the perimeter of the cylinder was free. The periodic length of each cylinder was three times its diameter (131 544 atoms). In what follows, these cylinders will be referred to as "as-carved". We focus on cylinders with the cylinder axis (z) parallel to the ⟨111⟩ direction of the fcc crystal, since we[14] previously showed that cylinders compressed along ⟨001⟩ and ⟨011⟩ axis exhibit buckling and folding instabilities that interfere with slip nucleation. For the simulations performed at 300, 400, and 500 K, the cylinders were equilibrated for 500, 400, and 200 ps, respectively, prior to the compression along the z-axis. For simulations performed below 300 K, the sample was annealed at 300 K for 200 ps and cooled at a rate of 500 K/ns. The initial length of each cylinder was scaled according to the temperature-dependent bulk lattice parameter. After thermal equilibration, the cylinders were deformed in compression by homogeneously rescaling the z-coordinates of all atoms. The rescaling factor was chosen to maintain a constant true strain rate of 1.351×10^{-4} ps^{-1}. Prior to each rescaling step, the atomic virial stress, averaged over all of the atoms in the system, σ, was calculated. In addition, we also calculated the atomic virial stress averaged over internal atoms, σ^{in}. Internal atoms are defined as those with potential energy less than −3.8 eV in the as-carved, unrelaxed cylinder (the energies per atom in the perfect crystal are −3.924 and −3.90 eV for the GRS and CY potentials, respectively). This definition excluded approximately the two outermost shells of atoms from the stress calculation. Previous studies have shown that the atomic stresses in the two external layers of a nanowire are very different from those on internal atoms due to the effects of surface stress.[8] The atomistic aspects of slip nucleation were followed by tracking the q_6 bond order parameter[16] for each atom. This parameter allows one to distinguish between the local atomic symmetry of fcc, body-centered cubic (bcc), and hexagonal close packed (hcp) lattices. The SF left behind when the leading Shockley partial advances, as well as the SF ribbon between two Shockley partials, can be recognized by a double layer of atoms with hcp coordination.

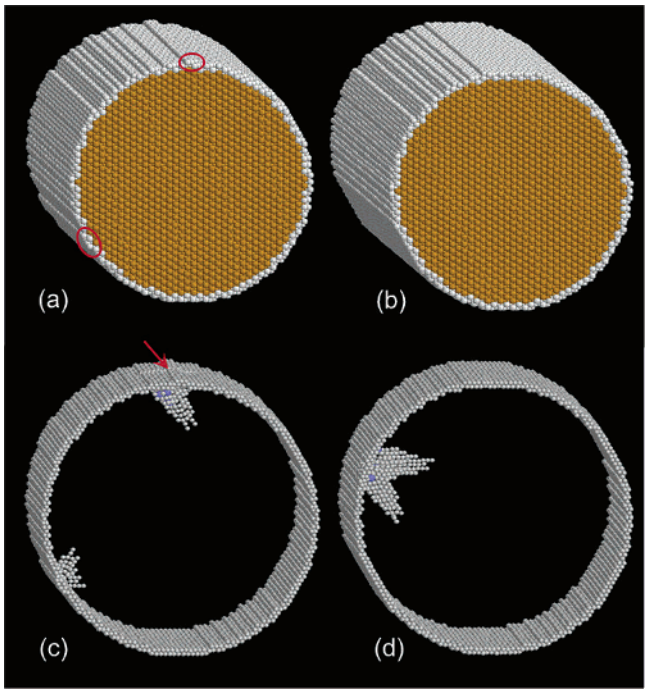

Figure 1. Atomic structures of (a) as-carved and (b) atomically polished nanopillars. The atoms are colored according to their bond order parameter, such that copper, blue, and white atoms have fcc, hcp, and distorted local coordination (i.e., first nearest neighbor symmetry that is not fcc, hcp, bcc, or icosahedral), respectively. The "atomically polished" cylinder was created by removing a total of 294 atoms ordered in ⟨111⟩ strings (marked by red ovals in (a)) from the "as-carved" cylinder. The atomic structure immediately following slip nucleation in configuration (a) is shown in (c). Drawing (d) shows the same thing for the atomically polished structure of (b). In (c) and (d), we do not show the atoms with fcc symmetry.

The atomic configuration at the onset of slip nucleation in the as-carved cylinder compressed at 2 K is shown in Figure 1c. For the sake of clarity, all atoms with fcc coordination are not shown in this figure. The groups of atoms with distorted coordination (white atoms) protruding toward the cylinder axis show the nucleation of dislocation half-loops. The atoms with hcp coordination (blue atoms) are precursors to SF nucleation. Figure 1c demonstrates clearly that slip nucleates in the vicinity of thin stripes of atoms, marked by red ovals in Figure 1a (consisting of several rows of atoms oriented along the cylinder axis, ⟨111⟩),

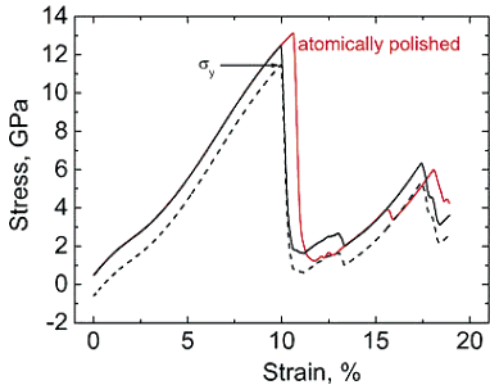

Figure 2. The stress−strain curves for as-carved (black lines) and atomically polished GRS nanopillars. The average atomic stress (averaged overall atoms) is shown as a dashed line and the internal stress (averaged over all atoms except those in the two outermost atomic shells) is shown as solid lines.

on otherwise flat terraces. The arrow in Figure 1c shows the position of a slip trace associated with the nucleation and motion of a Shockley partial into the cylinder. This trace (location where the dislocation nucleates) is centered around the three ⟨111⟩ atomic rows thick stripe of atoms. For all temperatures below 300 K examined, slip always nucleated in the vicinity of the marked ⟨111⟩ stripes. It should be emphasized that these stripes are aligned along the loading axis and cannot serve as stress concentrators for the present uniaxial load. This is interesting because earlier studies showed that the yield stress in nanowires was reduced in the presence of stress concentrators associated with the intersection of a SF with the surface[8] or full surface steps.[9]

To better understand the effect of the atomic structure of the surface on slip nucleation, we also performed a full set of MD simulations with smoother nanocylinders. We smoothed or polished the nanopillar in Figure 1a by removing the ⟨111⟩ stripes of surface atoms (Figure 1b) indicated by the red ovals (see Figure 1a). The atomically polished cylinders contained 131 250 atoms; i.e., only 294 atoms were removed. Despite the small number of atoms removed during polishing, the deformation behavior of the atomically polished cylinders was very different from that of their as-carved counterparts. For example, at 2 K slip nucleation in the as-carved and atomically polished cylinders occurred at the strains of 9.98% and 10.62%, respectively. This suggests that atomic polishing makes dislocation nucleation more difficult and increases the yield stress. The atomic configuration of the atomically polished cylinder at the onset of plasticity is shown in Figure 1d. A comparison of this figure with that for the as-carved cylinder (Figure 1c) indicates that removing the thin ⟨111⟩ stripes changes the location of slip nucleation at the surface.

Figure 2 shows the internal stress (σ^{in})−strain relation for the as-carved and atomically polished GRS cylinders compressed at 2 K. The dependence of the atomic stress averaged for all of the atoms in the as-carved cylinder on strain is shown by the dashed line. For the sake of convenience, we make the unconventional choice of the sign of the stress and strain; i.e. compressive stresses correspond to positive σ. The elastic parts of the stress−strain curves are nonlinear, which is associated with the high absolute values of stress. These elastic parts are almost identical for as-carved and atomically polished cylinders. An abrupt drop of stress indicates the onset of slip nucleation. Examination of the microstructure of the cylinders immediately after slip nucleation shows that a single nucleation event is rapidly followed by a further dislocation nucleation at different locations on the surface. It is this rapid succession of dislocation nucleation events that causes the large stress drop observed in the stress−strain curve. The subsequent, smaller stress drops mark individual slip nucleation events and slip propagation across the cylinder. At approximately 50 ps after initial yield, the cylinder microstructure is characterized by a high density of Shockley partials, some followed by trailing Shockley partials. After ∼100 ps, the density of lone Shockley partials diminishes, leaving mainly leading/trailing Shockley partial pairs. This is associated with the fact that for compressive deformation of the cylinders along the ⟨111⟩ direction, the Schmid factor for a leading Shockley partial (0.16) is lower than that for the trailing one (0.31).[8,14] This implies that the leading Shockley partial is swiftly followed by a trailing one. After ∼200 ps from the original slip nucleation event, the density of the dislocations in the cylinder goes to zero (i.e., the cylinders are perfect), albeit with a surface marred by slip steps and with some mono- and divacancies inside the cylinders. It is remarkable that all subsequent slip nucleation events in these cylinders with slip steps on the surface occur at much lower stresses than the initial slip nucleation. This again suggests that dislocation nucleation occurs preferentially (and at lower stress) near nonuniformities in the surface structure.

Figure 2 clearly demonstrates that slip nucleation in the atomically polished cylinder occurs at higher internal stresses than in the as-carved one. Repeated MD simulation runs showed that this difference in stresses is reproducible and is certainly above statistical fluctuations in the yield stress. Since the nonlinear elastic behavior is identical in the as-carved and atomically polished cases, the Schmid factors in both cylinders are identical at identical strains. This, in turn, means that slip in the atomically polished cylinder nucleates at larger values of the resolved shear stress in the interior than in the as-carved one. This indicates that for slip nucleation, the local atomic configuration at the surface is more important than the average value of the resolved shear stress in the interior of the cylinder. This conclusion is in contrast to the suggestion in ref 8. Note that the change in the surface structure that occurs upon atomic polishing does not lead to the formation or removal of stress concentrations. Therefore, the effect of surface structure modification on the yield stress is not associated with stress concentrators but rather some other aspect of the surface structure.

The idea that the resolved shear stress is the only factor controlling slip nucleation is based upon the assumption that slip nucleates in the interior of cylinder at some distance form the surface, where the effects of surface stresses are negligible. Our results, presented in Figure 2, clearly demonstrate that a minor change in surface structure, which has no effect on resolved shear stress in the interior,

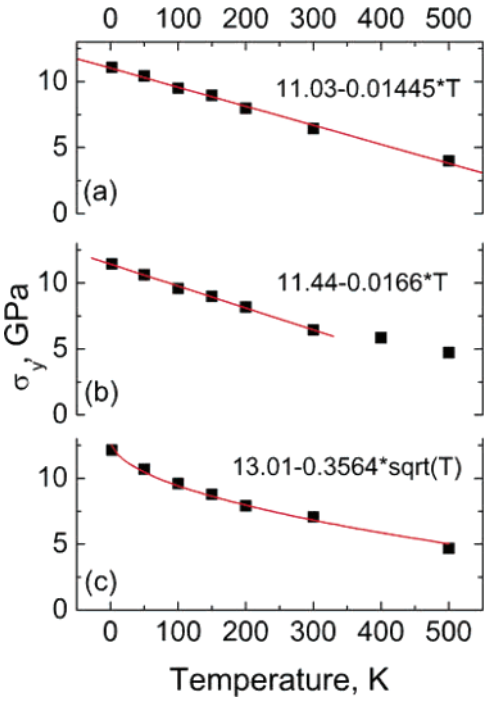

Figure 3. The temperature dependence of the yield stress for (a) the as-carved CY nanopillars, (b) the as-carved GRS nanopillars, and (c) the atomically polished GRS nanopillars.

significantly retards slip nucleation. This is convincing proof that slip nucleation is essentially a surface phenomenon.

The dependence of the atomic stress, averaged over all atoms (σ) in the as-carved cylinder, on strain is shown in Figure 2 by a dashed line. The initial value of stress at zero strain is negative (tensile) because of the effect of surface stress. This means that relaxing the periodic boundary conditions along the cylinder axis would lead to spontaneous contraction of the cylinder.[17] This means that the surface stress simply shifts the stress−strain curve uniformly downward. In what follows, we designate that maximum stress on the stress (σ)−strain curve (i.e., before the first stress drop) as the yield stress, σ_y.

Figure 3 shows the dependencies of σ_y on temperature, T, for the as-carved CY and GRS cylinders and for the atomically polished GRS cylinders. In the case of the CY potential (Figure 3a), the dependence is linear over the entire range of temperatures examined (2−500 K). In the case of the as-carved GRS cylinder, σ_y is a linear function of temperature in the 2−300 K range (the values of σ_y at higher temperatures deviate upward from the extrapolation of the straight line fitted to the low-temperature data). For the atomically polished cylinder, σ_y varies with temperature in a parabolic manner; $\sigma_y = A - BT^{1/2}$, where A and B are constants. On comparison of parts b and c of Figure 3, it is clear that atomic polishing, which removes only ~0.2% of the cylinder atoms, has a profound effect on the temperature dependence of σ_y. It should be also noted that at low temperatures, the yield stress associated with the atomically polished cylinder is larger than that for the as-carved one by more than 10% (in cylinders described by the same EAM potential).

To understand the effect of the interatomic potential and atomic polishing on the temperature dependence of σ_y, the atomistic mechanisms of slip nucleation should be considered in detail. It is tempting to describe slip nucleation in terms of classical nucleation theory, with the critical nucleus being a leading Shockley partial half-loop originating at the surface.[8] The positive contributions to the energy of this nucleus are provided by the Shockley partial core energy, its elastic energy, the energy of the SF left behind, and the energy of the corresponding surface step, while the driving force for nucleation is the mechanical work performed by the external force compressing the cylinder. A detailed quantitative analysis of this energy balance for nucleation (presented elsewhere[14]) showed that the contribution from the Shockley partial core dominates all other positive contributions to the nucleus energy. This means that surface morphology should have little effect on the energy barrier for slip nucleation. This is in contradiction with the results of the present work and with the results of other studies.[8,9] Most probably, the critical condition for nucleation involves a collective displacement of a group of near-surface atoms that cannot be described in terms of a well-defined dislocation. In our earlier work,[14] we suggested a phenomenological model in which the nucleation of the first Shockley partial at the surface of a nanopillar occurs at a critical strain at the surface, ϵ_c, which includes contributions from thermal vibrations, ϵ_{therm}, and elastic loading. This model was inspired by the Lindemann criterion for melting, which states that the ordered crystal melts at the temperature at which the average amplitude of atomic thermal vibrations exceeds 0.15 of a lattice spacing.[17] Assuming that the elastic (albeit nonlinear) initial part of the stress−strain curve is a monotonically increasing function of strain, $\sigma = f(\epsilon)$, we arrive at the following expression for σ_y

$$\sigma_y = f(\epsilon_c - \epsilon_{therm}) \quad (1)$$

The temperature dependence of σ_y can be attributed both to the temperature dependence of the function $\sigma = f(\epsilon)$ (which in the linear elastic limit corresponds to the temperature dependence of the Young modulus) and to the temperature dependence of ϵ_{therm}. Analysis of the simulated stress−strain curves shows that the relative variations of the function $\sigma = f(\epsilon)$ with temperature (between 2 and 500 K) do not exceed 11% for the GRS potential and 33% for the CY potential. This is much less than the temperature variations of σ_y (see Figure 3), and therefore, it can be concluded that it is the temperature dependence of ϵ_{therm} that dominates the variation of σ_y with temperature. The thermal strain ϵ_{therm} can be represented as $\Delta_{therm}/a(T)$, where Δ_{therm} and a are the absolute average amplitude of the thermal vibrations of the atoms (standard deviation of the positions) and the lattice parameter, respectively. The relative variation of the latter, in the temperature range of 2−500 K, does not exceed 1% and can safely be neglected. In order to determine the average vibration amplitude of surface (bulk) atoms, we measured the mean positions and standard deviations from these positions for 459 surface (294 bulk) atoms over 100

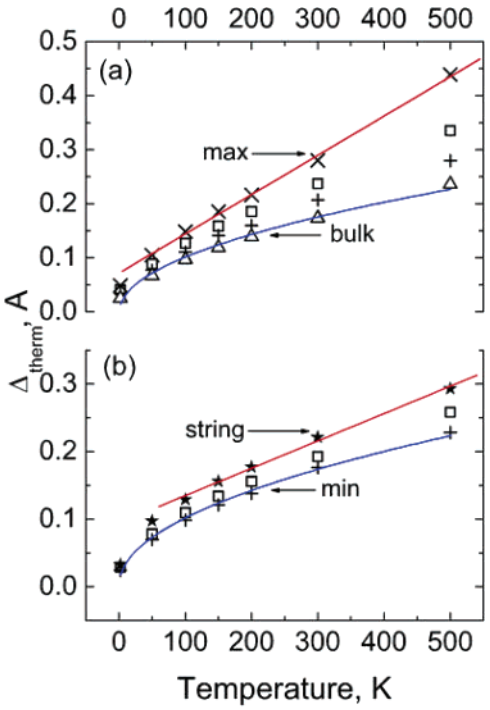

Figure 4. The thermal vibration amplitude vs temperature for the as-carved nanopillars. (a) Results for the CY nanopillars, where ×, □, and + correspond to the maximum, average, and minimum values of the vibration amplitude of surface atoms and △ to the vibration amplitude of bulk atoms. (b) Results for the GRS nanopillars, where ★ corresponds to the vibration amplitudes of atoms in the ⟨111⟩ atomic stripes and the other symbols are as per (a).

ps. The temperature dependence of Δ_{therm} for the surface and bulk atoms is shown in Figure 4. For the GRS potential case, we focus on the atoms within the surface stripes (see Figure 1a), near where dislocations nucleate. For the CY cylinders, dislocations nucleate at random locations, so we focus on the maximum values of the vibration amplitude. Figure 4a demonstrates that the maximal average vibration amplitude of selected surface atoms is a linear function of temperature in the 50−500 K range. At the same time, the temperature dependence of vibration amplitude of the bulk atoms exhibits a parabolic dependence on temperature $AT^{1/2}$, where A is a constant. For the as-carved GRS cylinders, the vibrational amplitude for the atoms within the ⟨111⟩ stripes varies linearly with temperature in the 100−500 K range. Interestingly, the vibration amplitude of the surface atoms that vibrate the least shows a parabolic temperature dependence, $AT^{1/2}$.

Since the temperature dependence of $\sigma = f(\epsilon)$ (see eq 1) is significantly weaker than that of Δ_{therm} (and, consequently, ϵ_{therm}), the temperature dependence of σ_y should mirror that of Δ_{therm}. Examination of Figures 3 and 4 supports this assertion. The linear decrease of σ_y with increasing temperature for the as-carved CY cylinders correlates well with the linear increase of the maximal value of Δ_{therm} with increasing temperature. Similarly, the linear decrease of σ_y with increasing temperature for the as-carved GRS cylinders (2−300 K), correlates well with the linear increase of Δ_{therm} (calculated for the ⟨111⟩ stripes of surface atoms). The differences between the temperature dependences of σ_y and Δ_{therm} at low temperatures (below 50 and 100 K for the CY and GRS potentials, respectively) may be related to the efficacy of the thermostat in dissipating the energy associated with the discrete compression steps that occur during the MD simulations.

A careful inspection of the atomic structure of the as-carved GRS cylinders shows that at 400 and 500 K sufficient surface diffusion occurs to disrupt the long-range order of the ⟨111⟩ stripes of surface atoms. This is why, at these temperatures, slip can nucleate at locations other than stripe edges. Since nucleation at other locations may be more difficult, σ_y tends to deviate upward from the linear extrapolation of $\sigma_y(T)$ from lower temperatures. The atoms in the most isolated stripes (i.e., thin stripes on large flat terraces) on the surfaces of the as-carved cylinders are particularly weakly bound to the surface. As a result, these atoms exhibit the largest values of Δ_{therm}. The removal of these atoms in the atomic polishing process leads to surfaces for which the maximal Δ_{therm} is smaller than that on the as-carved surfaces. In fact, the atoms that survive the atomic polishing process have values of Δ_{therm} that are very close to the smallest values on the entire surface (see Figure 4b). The temperature dependence of Δ_{therm} for these surface atoms is parabolic over the entire range of temperatures examined. This correlates well with the parabolic temperature dependence of σ_y for the atomically polished cylinders. This correlation between the temperature dependencies of σ_y and Δ_{therm} supports our hypothesis that it is a critical value of the net atomic strain at the surface, rather than the CRSS in the nanopillar interior, that should be achieved for slip nucleation.

The parabolic temperature dependence of Δ_{therm} is consistent with a simple harmonic model for thermal vibrations of atoms in solids. In this model, atoms vibrate around their equilibrium positions in the parabolic potential wells, independent of one another. This implies $\Delta_{therm} \propto T^{1/2}$. If the same model is also valid for surface atoms, the temperature dependence of Δ_{therm} should follow the same parabolic law, albeit with a larger coefficient of proportionality. In the literature, this effect is often discussed in terms of a lowering of the Debye temperature for surface atoms.[18] The behavior of the majority of the surface atoms in the GRS cylinders can be understood in this way. Weakening of the bonds between surface atoms and the underlying solid would produce larger vibration amplitudes, and therefore the role of anharmonicity in these vibrations will increase.[19,20] This anharmonicity can lead to a stronger temperature dependence, i.e., $\Delta_{therm} \sim T^n$ where $n > 1/2$. This is the case for most the surface atoms in the CY cylinders and for the atoms in the ⟨111⟩ stripes in the GRS cylinders. For these atoms, the binding to the surface is low and the temperature dependence of Δ_{therm} is nearly linear.

The connection between the temperature dependences of the yield stress and the atomic vibration amplitude (on average), together with the recognition of the effect of anharmonicity on the latter, helps us understand the effect of surface morphology on the mechanical behavior of

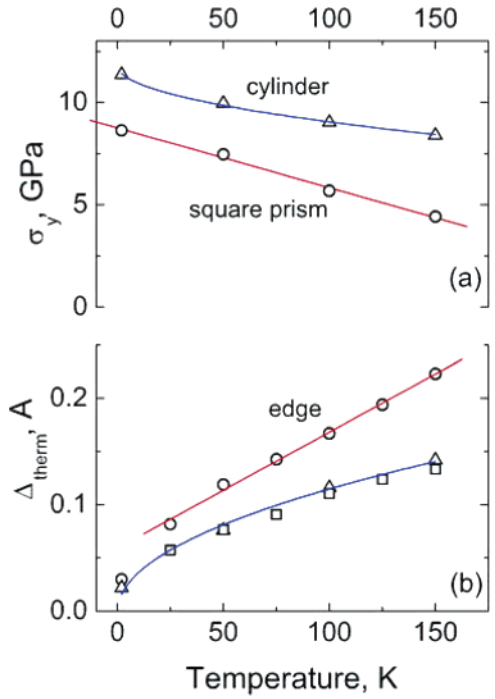

Figure 5. The temperature dependence of the (a) yield stress and (b) average vibration amplitude for the cylindrical and square prism GRS nanopillars. Squares and triangles in (b) denote the average vibrations amplitudes for a surface atom at the center of a face of the square prism nanopillar and for an atom, chosen at random, from those on the cylindrical nanopillar surface, respectively.

nanopillars more clearly. For example, slip nucleation at the edges of a nanowire of square cross section observed in simulations of Diao et al.[8] can be associated with the high average vibration amplitude of atoms/decreased binding of the atoms on the edges of the nanowire. To illustrate this point, we performed a series of MD simulations of ⟨111⟩-oriented cylindrical and square prism GRS nanopillars of aspect ratio 1:3 (containing 9248 and 9724 atoms, respectively). The as-carved cylindrical nanopillar did not exhibit any narrow atomic stripes on the surface. These nanopillars were deformed in compression at the same deformation rate used in the MD simulations described above (i.e., 1.351×10^{-4} ps^{-1}). The square prism nanopillars were equilibrated at the same temperature at which the compression tests were performed, in order to avoid the rounding of the edges by surface diffusion (i.e., below 200 K). Figure 5a demonstrates that σ_y is a linear function of temperature (2−150 K) for the square prism nanopillar and parabolic for the cylindrical nanopillar. Figure 5b shows that Δ_{therm} for a randomly selected atom on the square prism edge is a linear function of temperature (25−150 K), while Δ_{therm} for an atom in the center of a face of the prism is a parabolic function of temperature (as it is for surface atoms on the cylinder prism). Comparison of parts a and b of Figure 5 shows that there is, again, a close relationship between the yield stress and the average thermal vibration amplitude: it is the latter that determines the former. Another important conclusion that can be drawn from the comparison of the mechanical behaviors of cylindrical and square prism nanopillars is that the presence of sharp edges on the surface significantly decreases the value of σ_y. In fact, the presence of the edges in the square prism case leads to a drop in the yield stresses by about a factor of 2 at 150 K.

In the present work, we employed the periodic boundary conditions along the *z*-axis of the simulated cylinders and prisms. If the cylinders were truncated at a finite length, the tops and bottoms of the cylinders would have sharp edges around their periphery, while the prisms would also have sharp corners. As we have shown in this study, the average thermal vibration amplitude of atoms at sharp edges is higher than on the flat surface. It is obvious that the bonds of these periphery atoms would have to the rest of the crystal would be weaker than the corresponding bonds of the edge atoms or atoms on the flat facets. Therefore, replacing the periodic boundary conditions along the *z*-axis by terminating the rods would weaken both the cylinders and the prisms and shift the locations of slip nucleation toward their free ends. Indeed, in the recent atomistic simulations of the surface stress driven reorientation of gold nanowires, it was shown that surface-stress-induced slip nucleation in free-standing ⟨100⟩-nanowires occurred almost instantaneously at the nanowire ends.[21]

We return now to the effect of size on the compressive strength of gold nanopillars. In the experimental work of Nix and co-workers[5,6] the strength of the single crystalline pillars increased monotonically with decreasing diameter, for diameters ranging from several micrometers to about 300 nm. This was associated with the diminishing role of pre-existing dislocation and of strain hardening (which stems from interactions between the dislocations) and the increasing role of dislocation nucleation in deformation. Our atomistic computer simulations of as-carved ⟨111⟩ GRS nanopillars with diameters ranging from 2.5 to 10 nm revealed a strongly non-monotonic dependence of σ_y on diameter.[22] It was shown that the minima of σ_y are associated with the thin ⟨111⟩ atomic stripes similar to those removed by atomic polishing in the present work. The presence and the width of such stripes are determined by the discrete atomic nature of the nanopillars. This striking difference in the size effect on compressive strength of sub-micrometer and truly nanometer pillars underlines the importance of fine atomic scale surface features on the deformation of nanometer-sized objects or features.

In summary, we have shown that criterion for slip nucleation in single-crystal nanopillars is very different than that for macroscopic metallic single crystals. For the bulk material, the CRSS must be surpassed in order for plastic deformation to occur. In the case of nanopillars, slip (Shockley partial) nucleation occurs when a critical atomic strain at the surface is surpassed. The largest thermal strains occur where surface atoms are most loosely bound to the underlying material, such as at edges or in isolated atomic stripes. Consequently, these special locations serve as slip nucleation sites. The temperature dependence of the yield stress is determined by the temperature dependence of the average vibration amplitude of these loosely bound atoms. We have demonstrated that removing the loosely bound atoms (atomic polishing) leads to an increase in the stress

required for slip and a change in the temperature dependence of the yield stress from linear to parabolic.

Acknowledgment. This work was supported by the Princeton Center for Complex Materials funded by National Science Foundation (Grant Number DMR-0213706). E.R. wishes to thank the partial support of the Russell Berry Nanotechnology Institute at the Technion. Helpful discussions with Professor W. Soboyejo and Dr. H.-S. Nam are gratefully acknowledged.

References

(1) Wu, B.; Heidelberg, A.; Boland, J. J. *Nat. Mater.* **2005**, *4*, 525.
(2) Weihs, T. P.; Hong, S.; Bravman, J. C.; Nix, W. D. *J. Mater. Res.* **1988**, *3*, 931.
(3) Van Swygenhoven, H.; Derlet, P. M.; Froseth, A. G. *Acta Mater.* **2006**, *54*, 1975.
(4) Gouldstone, A.; Van Vilet, K. J.; Suresh, S. *Nature* **2001**, *411*, 656.
(5) Uchic, M. D.; Dimiduk, D. M.; Florando, J. M.; Nix, W. D. *Science* **2004**, *305*, 986.
(6) Greer, J. R.; Oliver, W. C.; Nix, W. D. *Acta Mater.* **2005**, *53*, 1821.
(7) Savitskii, E. M.; Prince, A. *Handbook of Precious Metals*; Hemisphere Publishing Co.: New York, 1969; pp 128−129.
(8) Diao, J.; Gall, K.; Dunn, M. L. *Nano Lett.* **2004**, *4*, 1863.
(9) Hyde, B.; Espinosa H. D.; Farkas, D. *JOM* **2005**, *57* (9), 62.
(10) Brochard, S.; Beauchamp, P.; Grilhe, J. *Phys. Rev. B* **2000**, *61*, 8707.
(11) Cai, J.; Ye, Y. Y. *Phys. Rev. B* **1996**, *54*, 8398.
(12) Grochola, G.; Russo, S. P.; Snook, I. K. *J. Chem. Phys.* **2005**, *123*, 204719.
(13) Cha, P.-R.; Srolovitz, D. J.; Vanderlick, V. K. *Acta Mater.* **2004**, *52*, 3983.
(14) Rabkin, E.; Nam, H.-S.; Srolovitz, D. J. *Acta Mater.*, in press.
(15) Frenkel, D.; Smit, B. *Understanding Molecular Simulations*, Academic Press: San Diego, CA, 2002.
(16) Steinhard, P. J.; Nelson, D. R.; Ronchetti, M. *Phys. Rev. B* **1983**, *28*, 784.
(17) Lindemann, F. A. *Phys. Z.* **1910**, *11*, 609.
(18) Nascimento, V. B.; Soares, E. A.; de Carvalho, D. E.; Lopes, E. L.; Paniago, R.; de Castilho, C. M. C. *Phys. Rev. B* **2003**, *68*, 245408.
(19) Häkkinen, H.; Manninen, M. *Phys. Rev. B* **1992**, *46*, 1725.
(20) Al-Rawi, A. N.; Kara, A.; Rahman, T. S. *Phys. Rev. B* **2002**, *66*, 165439.
(21) Diao, J.; Gall, K.; Dunn, M. L.; *Phys. Rev. B* **2004**, *70*, 075413.
(22) Rabkin, E.; Srolovitz, D. J. To be published.

NL0622350